engineering proceedings

MDPI

Proceeding Paper

Lunar Navigation System ODTS Signal in Space Error Analysis †

Cosimo Stallo [1,*], Carmine Di Lauro [1], Mattia Carosi [1], Laura De Leo [1], Martina Cappa [1], Daniele Musacchio [1], Daniele Cretoni [1], Henno Boomkamp [2], Pietro Giordano [3], Richard Swinden [3] and Javier Traveset [3]

[1] Thales Alenia Space Italy (TAS-I), 00131 Rome, Italy; carmine.dilauro@thalesaleniaspace.com (C.D.L.); mattia.carosi@thalesaleniaspace.com (M.C.); laura.deleo@thalesaleniaspace.com (L.D.L.); martina.cappa@thalesaleniaspace.com (M.C.); daniele.musacchio@email.com (D.M.); daniele.cretoni@thalesaleniaspace.com (D.C.)
[2] Telespazio Germany (TPZ), 64293 Darmstadt, Germany; henno.boomkamp@telespazio.de
[3] European Space Agency (ESA), 2200 Noordwijk, The Netherlands; pietro.giordano@esa.int (P.G.); richard.swinden@esa.int (R.S.); javier.ventura-traveset@esa.int (J.T.)
* Correspondence: cosimo.stallo@thalesaleniaspace.com
† Presented at the European Navigation Conference 2023, Noordwijk, The Netherlands, 31 May–2 June 2023.

Abstract: In recent years, the Moon has gained renewed interest in terms of human exploration for scientific purposes. In this context, Thales Alenia Space is leading a consortium to define the main concepts for a Lunar Radio Navigation System (LRNS) in terms of Orbit Determination and Time Synchronization (ODTS) as part of an ESA Technology Development Element (TDE) programme. This work focuses on the latest performance results achieved through a dedicated simulator in terms of Signal In Space Error (SISE).

Keywords: Signal In Space Error (SISE); Orbit Determination and Timing Synchronisation (ODTS); Lunar Radio Navigation System (LRNS)

Citation: Stallo, C.; Di Lauro, C.; Carosi, M.; De Leo, L.; Cappa, M.; Musacchio, D.; Cretoni, D.; Boomkamp, H.; Giordano, P.; Swinden, R.; et al. Lunar Navigation System ODTS Signal in Space Error Analysis. *Eng. Proc.* **2023**, *54*, 37. https://doi.org/10.3390/ENC2023-15468

Academic Editors: Tom Willems and Okko Bleeker

Published: 29 October 2023

1. Introduction

In recent years, lunar missions have been attracting renewed interest, in the clear perspective of achieving the required technologies and capabilities necessary to expand the human presence in the solar system [1,2]. Unlike the first race to the Moon in the 1960s, this return is aimed to be effective and permanent, so that more than a hundred missions are planned in the upcoming years, opening up new opportunities for both space agencies and private companies. Despite the high number of planned missions, no global lunar communication and navigation infrastructure is yet available, so every mission is currently planning its own custom solution to communicate and navigate using Earth-ranging or dedicated in situ relay capabilities. For this reason, the European Space Agency's (ESA) Moonlight initiative [3,4] aims to provide navigation and communication capabilities and services to establish a reliable, sustainable and scalable network, compatible with the LunaNet Framework [5].

This contribution will present an ODTS concept to implement the satellite synchronization and generation of the clock and ephemeris data required for the navigation message, as well as the performances achievable. To accomplish this, an ODTS tool capable of simulating the generation of the broadcasted navigation message, which contains information about the satellites' ephemeris and clock, has been developed. This study assumes a constellation of four satellites in Elliptical Lunar Frozen Orbits (ELFO) in order to achieve the highly accurate and reliable positioning of a user on the Moon South Pole (such as in [6,7]). The proposed baseline for LRNS orbit determination consists of Earth-based tracking techniques through Telemetry, Tracking, and Command (TT&C) links [8,9]. On the other hand, time synchronization will rely on the observation of on-board time provided by space-qualified atomic clocks with respect to a Master Clock on Earth through the means of Two-Way Time Transfer (TWTT) from exploiting the same TT&C link.

For what concerns the Time Synchronization (TS) analysis, a set of Monte Carlo (MC) simulations has been run to estimate the LRNS satellite onboard clock offset using two-way time transfer observables in a Kalman filter. On the other side, the orbit determination (OD) contribution has been evaluated in two ways: a first approach makes an assumption on the outputs of the OD process, while the second one performs a Monte Carlo analysis. The final results are then compared with the requirement to drive conclusions.

The work performed in this study has been financed under the ESA TDE program and applies to a generic lunar radio navigation system, thus it is not necessary to represent what the Moonlight programme will implement. In addition, it does not apply the Moonlight service performance requirements defined by ESA as part of the Moonlight programme invitation to tender.

The paper is structured as follows: Section 2 provides a description of the system architecture of this satellite system; Section 3 provides a description of the SISE error and details the simulations performed to assess its 95% value as a function of the Age Of Data (AoD). Finally, Section 4 reports the main conclusions.

2. LRNS ODTS System Architecture

On the basis of the previous results achieved in [8,9], the final ODTS system baseline foresees the following elements for Space Segment and Ground Segment.

2.1. Space Segment

For the OD process, LRNS satellites will carry onboard an X-band multi-functional Code Division Multiple Access (CDMA) transponder that will be used for TT&C, Ranging and Time Synchronization, one High Gain Antenna (HGA) for normal mode and two Low Gain Antennas (LGA) for contingency operations, and a passive Satellite Laser Ranging (SLR) retroreflector for independent validation.

Concerning time keeping, three mini-RAFS (Rubidium Atomic Frequency Standard clocks) with a combination unit will be available onboard. These clocks will generate a free-running time scale initialized to the LRNS Reference Time (LRT), while asynchronous two-way time transfer is exploited on the same TT&C link used for OD.

The key advantage of this concept is that both OD and TS make use of the same TT&C Deep Space Transponder (DST) and related antennas and HPA.

2.2. Ground Segment

The LRNS ground segment includes three dedicated TT&C stations (a 90 cm diameter dish for normal mode in Multiple Spacecraft Per Antenna (MSPA) approach [9], and at least a 5 m diameter dish for contingency mode per site) at a longitudinal separation of around 120° to obtain global coverage. The stations must be endowed with an internal delay calibration system in the X band to calibrate the excess delay due to the ground station ranging measurement equipment. Moreover, SLR tracking will be provided by the International Laser Ranging Service on a best-effort basis.

The ground TS architecture is based on a network of ground stations synchronized via the Stand-Alone-All-in-View GNSS TS technique [10,11], including a master clock station in charge of generating the LRNS Reference Time.

3. SISE Analysis

An ODTS simulator has been developed to reproduce the generation and transmission of the broadcasted navigation message, containing information about the satellites' ephemeris and clock. Within the LRNS project context, the SISE is defined in line with the LunaNet Interoperability Specification [5] as the instantaneous difference between the position, velocity, and time of an LRNS satellite as broadcasted by the LRNS navigation message, and the true satellite position, velocity, and time, respectively, expressed in the lunar reference frame and the lunar time system standard. The SISE can be expressed for convenience in two parts:

1. Signal-In-Space Error for positioning ($SISE_{pos}$), according to Equation (1), where x, y, z, and t are the true position and time, while the corresponding tilde represent the values broadcasted in the navigation message.
2. Signal-In-Space Error for velocity ($SISE_{vel}$) according to Equation (2), where $\dot{x}$, $\dot{y}$, $\dot{z}$, and $c\dot{t}$ represent the velocity and clock drift, while the corresponding tilde are the values broadcasted in the navigation message.

Within this project, an initial SISE target value of 25 m at 95% (this activity has been performed prior to the publication of the ESA Moonlight ITT and the related ESA Service Requirement Document (ESRD), so the SISE target value here considered is not the final one in the Moonlight ESRD) has been proposed by ESA and will be used as reference for the performance assessment.

$$SISE_{pos} = \sqrt{\left(x - \tilde{x}\right)^2 + \left(y - \tilde{y}\right)^2 + \left(z - \tilde{z}\right)^2 + \left(ct - c\tilde{t}\right)^2}, \quad (1)$$

$$SISE_{vel} = \sqrt{\left(\dot{x} - \tilde{\dot{x}}\right)^2 + \left(\dot{y} - \tilde{\dot{y}}\right)^2 + \left(\dot{z} - \tilde{\dot{z}}\right)^2 + \left(\dot{ct} - \tilde{\dot{ct}}\right)^2}, \quad (2)$$

The following sections will present the approach proposed for the time synchronization and the orbit determination simulations.

3.1. TS Error Budget for SISE Derivation

A TS simulator is implemented around the TS baseline system architecture described in [8–10] and summarized in previous paragraphs, to simulate the TS concept designed and compute the accuracies achieved. To reach its purpose, it reproduces the real satellite on-board clock offset and the ones resulting from the TWTT observables collection. These are then exploited in the implemented Kalman Filter (KF) to derive the three clock corrections (time offset—a_{f0}[s], frequency offset—a_{f1}[s/s], and frequency drift—a_{f2}[s/s^2]) which, broadcasted to a user in the navigation message, allow it to predict the satellite on-board clock offset. Based on them, the simulator computes the SISE Clock Error, the difference between the real and estimated clock offset. The TS simulator process is summarized in the following steps:

1. Simulation of the real satellite on-board clock offset w.r.t. Lunar Reference Time (LRT).

The on-board clock behaviour is reproduced by the time-dependent Equation (3). The model includes: a deterministic timing error expressed by a quadratic polynomial equation, a random noise error generated according to [11], and a thermal sensitivity variation result of a sinusoidal temperature variation profile.

$$x_0(t) = a_{f0} + a_{f1}(t - t_0) + \frac{1}{2} \cdot a_{f2}(t - t_0)^2 + \varepsilon(t - t_0) + Th_v(t - t_0), \quad (3)$$

The clock offset coefficients, the clock noise parameters and the thermal sensitivity intervening, respectively, in the three frequency deviations are selected properly to reproduce miniRAFS technology behaviour. Moreover, the clock offset is reported with respect to the Master Clock timescale which defines the LRT for the constellation. Typical a_{f0}, a_{f1}, and a_{f2} parameters characteristic of an Active Hydrogen Maser (AHM) are considered to generate the reference.

2. Simulation of the Two-Way Time Transfer noise based on error budget.

To reproduce the residual error due to the TWTT, each contribution of noise on top the satellite on-board clock offset measurements is simulated as a Gaussian distribution with mean and standard deviation defined by a TWTT error budget. Table 1 summarizes the errors assessment conducted within this project [8–12].

Table 1. Two-Way Time Transfer residual error budget. The delay due to relativistic effects, crossing of troposphere, and earth rotation are considered as negligible.

Type of Residual Error	Description	Bias or Mean [ns]	Standard Deviation [ns]
Epoch-mismatch	Misalignment between the epochs timestamped on the basis of the local time reference. It is derived from the difference between ground and space clock error assuming conservative values of frequency offset: Ground Clock of 1×10^{-11} and Space Clock of 1×10^{-9}.	0.012	-
Ionospheric	Delay due to crossing of ionosphere. Computed through the equation below with f_{gs} = 7.22 GHz, f_{sg} = 8.45 GHz and an assumed worst case TEC = 1×10^{18} electrons/m^2. $\varepsilon_{iono} = 40.3 \times \frac{TEC}{c} \times \left(\frac{1}{f_{gs}^2} - \frac{1}{f_{sg}^2}\right)$	0.7	-
LRNS-Orbit	OD error in LRNS satellite position estimation, depending on OD error statistics. The proportionality is derived from the mean and standard deviation of the ephemeris error in the radial direction resulting from OD tool simulations.	$\propto$0.2	$\propto$4
Calibration	On-board group delay of hardware components. It is the accuracy reached considering the state-of-the-art TWSTFT protocol (1.4$\sqrt{2}$ ns = 2 ns) [13,14].	2	-
TWTT noise	Background white noise due to time transfer. Typical values of noise affecting the Time Transfers through a signal in space with the Two-Way technique [15].	-	0.75
Ground stations synchronization	Residual delay due to ground-to-ground TS to a Master Clock Station by GNSS timing RX [16]. Not included in measurements w.r.t. Master Clock Station. The assessed values are based on TASI background experience on GNSS timing RX available on the TASI timing laboratory (RF path timing chain) and by the on-going Galileo program.	7	0.5

The sum of error contributions are then exploited to derive three different overall TWTT random noise errors, one per each Ground Station.

3. Simulation of TWTT observables.

The TWTT observables result from the sum of the TWTT noises to the real clock offset. To be in line with the mission selected Time Transfer (TT) sessions, satellite visibility, and ground-to-ground calibration aspects, the 1s sampled components of the simulated measurements are further processed as follows:

- The observables of the 5 min time transfer session are averaged to provide one sample each 45 min (according to the baseline TT session, [12]);
- They are filtered through the visibility matrix that considers the time interval in which the selected satellite is in view of the selected ground station.
- They are pre-processed in a calibration window to remove the residual ground calibration bias from the observables collected w.r.t. Ground Clock Station.

4. Kalman Filter estimation of satellite on-board clock offset.

Due to its proved effectiveness in predicting and compensating clock offsets [17], a Kalman Filter is implemented in the simulator to obtain from noisy TWTT observables, which are known to have residual errors, the searched states (a_{f0}, a_{f1}, and a_{f2}).

After an initialization phase and fine tuning, a Dynamic State Model equation describing the dynamical evolution of the physical system in time is implemented, representing the prediction equation of the filter. At each step, the predicted states are updated through a weighted correction extrapolated from the comparison with the measurements (the collected TWTT observables). Since the TWTT baseline considers the collection of three observables, one per each Ground Station, a Kalman filter for multiple sensor system is

implemented: the Parallel Kalman Filter [18,19]. It updates the states once all measurements are processed. This computation gives, in output, the best reachable estimation of the satellite clock offset states (a_{f0}, a_{f1}, and a_{f2}) in the whole time window of simulation. These states are the clock parameters sent in the Navigation Message to the User Segment.

5. SISE Clock Error computing.

The SISE Clock Error is computed as the difference between the real and the estimated clock offset at a specific prediction time. The estimated value is derived by the clock offsets estimate, obtained as a product of the Kalman Filter, with the procedure described below. The computation starts at the end of the Kalman filter initialization process window and discards the first solution data comprised in the imposed Kalman filter warm-up period, since they are affected by high instabilities.

A configurable time window of 12 h is fixed to establish the amount of clock offset data for the least-squares estimation of the a_{f0}, a_{f1}, and a_{f2} parameters. The clock coefficients are then exploited to propagate in future batch of data the predicted clock offset. The propagation is realized at different prediction time, from 1 s to 12 h with a time span of 15 min. The predicted value at the end of the coverage time is finally compared with the real clock offset for the computation of the SISE clock prediction error.

The fitting and prediction time window is then translated to the next sample along the time window and the steps are repeated. SISE computation logic is summarized in Figure 1.

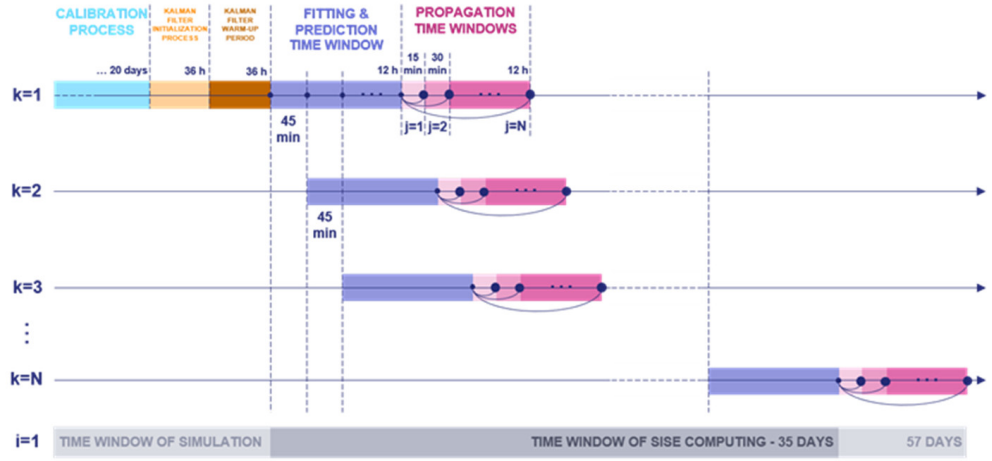

Figure 1. SISE Clock Error computation logic.

SISE Clock Error Results

The SISE Clock Error with a different Prediction Time of propagation (from 1 s to 12 h with a time span of 15 min) is obtained in Figure 1. A Monte Carlo based on 150 simulations applied on 1120 samples (one sample each 45 min in a time window of 35 days) for 49 different prediction times (for a total of 8.23×10^6 realizations) is applied.

The SISE Clock Error (shown in Figure 2) at 0 AoD is mainly due to the TWTT errors affecting the measurements. This noise distribution has a no zero mean value that has the major impact.

The SISE Clock Drift Error is computed with the same steps of the SISE Clock Error computing applied to the clock offset drift, a_{f1}. The Clock Drift Error, propagated at a specific prediction time, is compared to the real Clock Drift calculated as the first derivative of the simulated real on-board clock offset. The result is obtained in Figure 3.

Figure 2. SISE Clock Error evolution from TS software v4.0 Monte Carlo simulation.

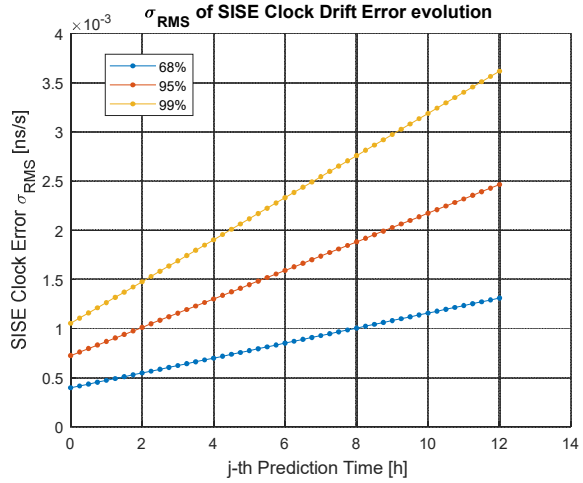

Figure 3. SISE Clock Drift Error evolution from TS software v4.0 Monte Carlo simulation.

Its value indicates how accurately we can predict the SISE Clock Drift at that specific propagation time.

These results are then merged with the OD error budget for the overall SISE derivation, as shown in Section 3.3.

3.2. OD Error Budget for SISE Derivation

In the framework of the LRNS project, the OD contribution to the SISE is estimated, acknowledging that it will vary under the influence of a large number of contributing factors such as the unpredictable variability in solar radiation pressure, deviations due to the difference between the real spacecraft attitude and the modelled one, unmodelled biases, and orbit estimation accuracy and mismodelling errors. Moreover, given that the navigation message broadcasted to the user is based on an orbit prediction, it is based on the numerical integration of the satellites' equations of motion, which suffer from input errors in the initial position X_0, initial velocity V_0, and acceleration model.

Two analysis methods will be shown to assess the SISE error, as defined above:

1. The first approach makes assumptions on the errors on X_0, V_0, and acceleration and computes the associated range of SISE errors from these, i.e., it makes assumptions directly on the outputs of the ODTS process.
2. The second approach makes an assumption on the input conditions to the ODTS process and runs a series of Monte Carlo simulations to vary the range of the SISE values.

3.2.1. SISE Derived from Assumptions on the Outputs of the ODTS Process

The orbit prediction is a fully deterministic process that follows the Newtonian equation of motion (Equation (4)):

$$X(t) = X_0 + V_0 t + \iint A(t) dt^2, \quad (4)$$

Therefore, the error in the predicted position is the linear sum of the errors in each of the three input errors presented above. Values for the three errors, based on early ODTS simulator results and data arcs with a length from 4 up to 6 days, have been provided as follows:

- Error in the initial position X_0 of 2 m
- Error in the initial velocity V_0 of 0.0002 m/s
- Error in the acceleration A(t) of 5×10^{-9} m/s^2

Monte Carlo simulations allow for re-assessing the assumptions, especially for X_0 and V_0.

As an example, Figure 4a shows how the initial position factor is varied over a range to obtain a bundle of curves with the "typical" value curve in the middle of each plot. Taking the lowest assumption for the three errors, a "best case" curve can be constructed, as well as a "worst case curve" can be obtained with the worst values for each errors.

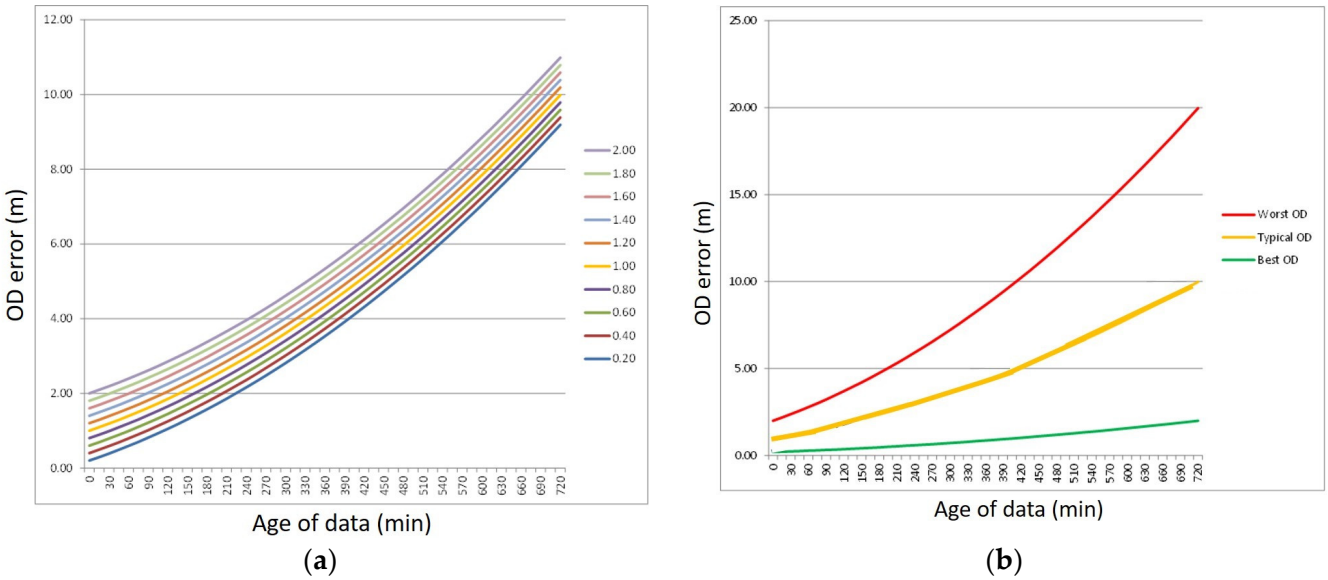

(**a**) (**b**)

Figure 4. (**a**) Orbit prediction error shown as function of different position errors X_0 and (**b**) SISE error as a function of the age of data for the OD process.

Finally, the total SISE error is obtained in Figure 4b. Derived from this analysis and assuming a normal distribution of errors varying between the worst case and best case, the expected SISE errors (3D position and clock combined) are reported in Table 2, from which we can derive that the SISE requirement of 25 m seems feasible with this approach.

Table 2. 95% and 99% SISE error levels as a function of the Age of Data (AoD).

	AoD 6 h	**AoD 12 h**
95% error level	7.6 m	18.4 m
99% error level	9.1 m	22.6 m

3.2.2. SISE Derived from Monte Carlo Analysis

As an alternative to the previous analysis, it is possible to vary some input assumptions to the OD simulator, simulate a truth orbit and tracking data, and run a series of OD solutions that cover the same period. The used assumptions are summarized in Table 3.

Table 3. Assumptions* made and impact on number of MC cases and actual number of simulations performed.

	Assumption	Units	Low	Typical	High	MC Factor	Accum.
Truth orbits	Solar activity	SFU	-	-	350	1	1
	Arc length	days	-	4.0	-	1	1
Data simulation	Lunar reference frame error	masec	0	-	1	2	2
	Range noise	m	0.05	-	0.5	2	4
	Range-rate noise	mm/s	0.00	-	0.10	2	8
	Range bias	m	-	1.00	-	1	8
	Data gaps (nr/max duration)	-/hrs	0/0	5/3	-	2	16
ODTS configuration	Arc length (overlap)	days	-	4.0/0.5	-	1	16
	Prediction interval	days	-	0.5	-	1	16
	SRP validity (Bernese 9p model)	days	1	daily	-	2	32
	One or both data types	-	-	Range only	both	2	64
	Observation sample interval	minutes	-	5	-	1	64
	Number of solution arcs	-	-	10	-	10	640
Message fit	Typical fit error RMS	m	-	0.2	-	1	640

* Most OD solutions without Doppler were ignored leading to a total number of simulations executed of 528.

In all cases, truth orbits were propagated with the best known dynamic models, using IERS standards and/or best practices (IGS/IERS). Furthermore, the errors in time synchronization do not have any impact on the orbit determination results, although they do affect the SISE. The overall length of a simulation in the analysis is given by the product of the number of solution arcs (10) by the length of each arc, which is assumed to be equal to 3.5 days. This means that a single simulation lasts 35 days and is made up of arcs of 3.5 days length. In order to evaluate the SISE, the last 12 h of each arc is assumed to be the predicted orbit part from which, in reality, the navigation message is generated.

The comparisons between the truth orbit and orbit available to the user were made in the three directions (radial, along-track, and cross track) separately, and 3D norm for position and velocity. With respect to the previous case, the orbit model is updated including a set of empirical harmonic accelerations at a frequency of one cycle per orbital revolution, to better simulate the dynamic model's imperfections. This practice is very common for spacecrafts that have a less than perfect dynamic model, such as uncalibrated surface force properties, and is therefore used for LRNS satellites. The result is that, if two orbit solutions for the same period are compared, the dominant error signal is typically an oscillation with a period of one orbit, because almost all dynamic models have some form of periodicity that is in phase with the orbit (e.g., the gravity field, the solar radiation pressure, and other surface forces).

In Figure 5, it is possible to see the SISE evaluated for position and velocity, respectively, with the 95% and 99% error levels, that follow the error envelope imposed by some of the least accurate cases. The figures show the point clouds resulting from the MC simulations described in Table 3 as a function of the age of data, that is, the time elapsed within the prediction interval upon which the orbit information is based.

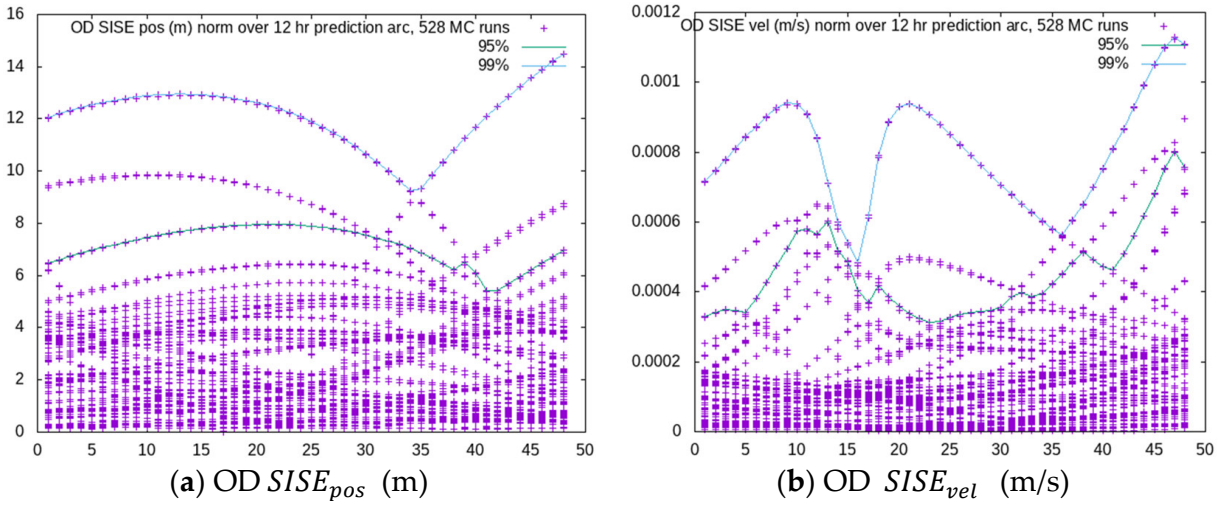

(**a**) OD $SISE_{pos}$ (m) (**b**) OD $SISE_{vel}$ (m/s)

Figure 5. OD SISE plots: (**a**) OD SISE for position (m) as a function of age-of-data (hrs) and (**b**) OD SISE for velocity (m/s) as a function of age-of-data (hrs).

Table 4 summarizes the expected SISE error levels for 95% and 99%, for position and velocity with OD and TS errors combined.

Table 4. SISE summary 95% and 99% error levels. Combination of OD&TS: 1 ns = 0.3 m.

		OD		TS		OD & TS Combined	
AOD	**Error Level**	**Position (m)**	**Velocity (mm/s)**	**Bias (ns)**	**Drift (s/s)**	**Pos + Bias (m)**	**Vel + Drift (mm/s)**
6 h	95%	7.9	0.33	57	2.20×10^{-3}	18.8	0.74
	99%	11.9	0.85	74	3.00×10^{-3}	25.2	1.24
12 h	95%	7.0	0.61	140	5.30×10^{-3}	42.6	1.70
	99%	14.5	1.10	182	7.40×10^{-3}	56.5	2.48

3.3. SISE Results Obtained by Combination of OD and TS Errors

The OD SISE results do not depend on the TS SISE values, but the clock estimation depends to some extent on the orbit accuracy. In fact, the TS algorithm receives, as inputs, the value of the OD error at the initial epoch of each simulation arc and the visibility matrix computed for each satellite and station pair. Nonetheless, the results for OD and TS are combined by the means of a root-sum-square approach, because a combination of the simulation results in a more direct way was not practical.

The SISE 95% and 99% are also shown in Figure 6, from which a 95% error level of about 6 m is obtained at the initial time, assessing that the initial assumption of a 2 m error was too optimistic. Because the OD errors now contain the once-per-orbit signals, the shape of these figures is no longer as simple as those in Figure 4, which are based on the assumption that the acceleration error is constant during the prediction interval. However, the most significant conclusion that can be drawn from the comparison of the two analysis methods is that they result in reasonably similar error levels, in the order of 20 m after 6 h, depending on the assumptions and input conditions.

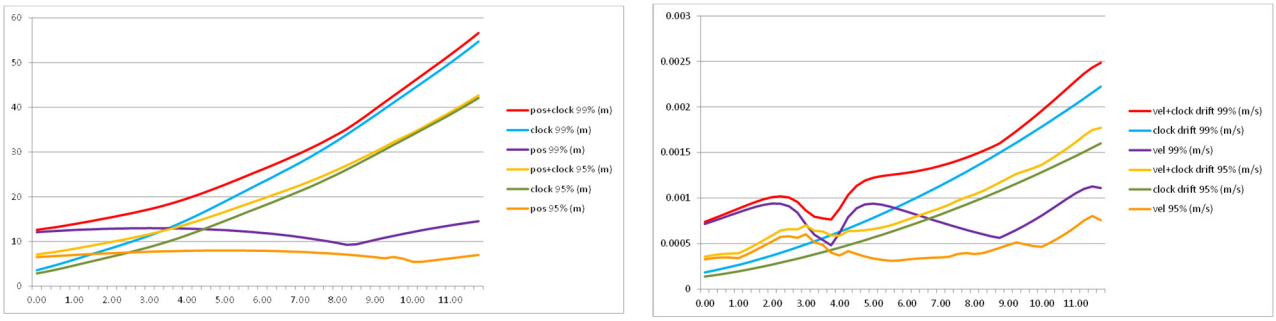

(**a**) (**b**)

Figure 6. SISE 95% and 99% error levels: (**a**) error levels for position (m) as a function of age-of-data (hours) and (**b**) error levels for velocity and clock drift (m/s) as a function of age-of-data (hours).

4. Conclusions

This study aimed at demonstrating the feasibility of the SISE requirements in terms of achievable ODTS performances, showing that good performances for target value of 25m at 95% are achieved in the first 6 h of Age of Data. In the frame of this study, an approach based on the outputs of the OD process and Monte Carlo style simulations showed the consistency of the employed simulator, since they achieved similar error levels. Concerning the TS error, the Monte Carlo approach allowed for obtaining a sufficiently large number of simulations to be used to drive a statistic and obtain a reliable error contribution. Although several factors still have to be considered at this stage of detailed design, the proposed ODTS baseline is considered as the best candidate for potential future lunar radio navigation systems.

Author Contributions: Conceptualization, C.S., C.D.L., M.C. (Mattia Carosi), L.D.L., D.M., P.G., R.S. and J.T.; methodology, C.S., C.D.L., M.C. (Mattia Carosi), L.D.L., D.M.; software, M.C. (Martina Cappa), D.C. and H.B.; validation, L.D.L.; formal analysis, C.S., D.C., M.C. (Martina Cappa) and H.B. ; investigation, C.S., C.D.L., M.C. (Mattia Carosi) and D.M.; resources, C.S., P.G., R.S. and J.T.; data curation, C.S., M.C. (Martina Cappa) and H.B.; writing—original draft preparation, L.D.L. and M.C. (Martina Cappa); writing—review and editing, L.D.L.; visualization, L.D.L.; supervision, C.S.; project administration, C.S. All authors have read and agreed to the published version of the manuscript.

Funding: This research was funded by ESA TDE study LRNS contract No. 4000135400/21/NL/CRS.

Institutional Review Board Statement: Not applicable.

Informed Consent Statement: Not applicable.

Data Availability Statement: Further data used in this study cannot be shared due to policy agreement between TAS-I and the other members of the consortium that have carried out this study.

Conflicts of Interest: The authors declare no conflict of interest.

References

1. International Space Exploration Coordination Group. The Global Exploration Roadmap. *January 2018.* Available online: https://www.globalspaceexploration.org/wordpress/wp-content/isecg/GER_2018_small_mobile.pdf (accessed on 28 October 2023).
2. Kaplan, S. *Eyes on the Prize. The Strategic Implications of Cislunar Space*; Center for Strategic & International Studies: Washington, DC, USA, 2020.
3. Grenier, A.; Giordano, P.; Bucci, L.; Cropp, A.; Zoccarato, P.; Swinden, R.; Ventura-Traveset, J. Positioning and Velocity Performance Levels for a Lunar Lander using a Dedicated Lunar Communication and Navigation System. *NAVIGATION J. Inst. Navig.* **2022**, *69*, navi.513. [CrossRef]
4. Schönfeldt, M.; Grenier, A.; Delépaut, A.; Swinden, R.; Giordano, P.; Ventura-Traveset, J. Across the Lunar Landscape: Towards a Dedicated Lunar PNT System. *Inside GNSS*. 2020. Available online: https://insidegnss.com/across-the-lunar-landscape-towards-a-dedicated-lunar-pnt-system/ (accessed on 27 November 2023).
5. LunaNet Interoperability Specifications. Available online: https://esc.gsfc.nasa.gov/static-files/LunaNet%2520Interoperability%2520Specification.pdf (accessed on 28 October 2023).
6. Ely, T.A. Stable constellations of frozen elliptical inclined lunar orbits. *J. Astronaut. Sci.* **2005**, *53*, 301–316. [CrossRef]

7. Ely, T.A.; Lieb, E. Constellations of elliptical inclined lunar orbits providing polar and global coverage. *J. Astronaut. Sci.* **2006**, *54*, 53–67. [CrossRef]
8. Stallo, C.; Zini, E.E.; Cretoni, D.; Tomasicchio, G.; Di Lauro, C.; Musacchio, D.; Boomkamp, H.; Ventura-Traveset, J.; Giordano, P.; Carosi, M.; et al. Candidate System concepts for a Lunar Satellite Navigation System. In Proceedings of the NAVITEC 2022, Online Event, 5–7 April 2022.
9. Stallo, C.; Di Lauro, C.; Carosi, M.; Zini, E.; Musacchio, D.; Cretoni, D.; De Leo, L.; Cappa, M.; Laurenti, M.; Boomkamp, H.; et al. Orbit Determination and Time Transfer in Selenodetic reference frames for a Lunar Radio Navigation System. In Proceedings of the 8th GNSS Colloquium, Sofia, Bulgaria, 14 September 2022.
10. Lombardi, M. Fundamentals of Time and Frequency. In *The Mechatronics Handbook 1.0-8493-0066-5*; CRC Press: Boca Raton, FL, USA, 2002; pp. 341–358.
11. Riley, W.J. *Handbook of Frequency Stability Analysis*; Special Publication 1065; NIST: Boulder, CO, USA, 2008.
12. Stallo, C.; Di Lauro, C.; Carosi, M.; Zini, E.; Musacchio; De Leo, L.; Cretoni, D.; Laurenti, M.; Boomkamp, H. Performance Analysis of Lunar Radio Navigation ODTS System. In Proceedings of the 2023 International Technical Meeting of the Institute of Navigation, Long Beach, CA, USA, 24–26 January 2023; pp. 190–203. [CrossRef]
13. Zhang, V.; Jiang, Z.; Fujieda, M.; Piester, D.; Esteban, H.; Matsakis, D.; Naumov, A. CCTF Working Group on Two-Way Satellite Time and Frequency Transfer. In: CCTF/17-23 (2017). Available online: https://www.bipm.org/documents/20126/28431178/working-document-ID-10203/527b697a-9394-f690-6cb5-c0992e201de7/ (accessed on 27 November 2023).
14. Piester, D.; Achkar, J.; Becker, J.; Blanzano, B.; Jaldehag, K.; de Jong, G.; Koudelka, O.; Lorini, L.; Ressler, H.; Rost, M.; et al. Whibberley: Calibration of Six European TWSTFT Earth Stations Using a Portable Station. In Proceedings of the 20th European Frequency and Time Forum, Braunschweig, Germany, 27–30 March 2006; pp. 460–467.
15. Michito, I. Precise Time and Frequency Transfer. *J. Natl. Inst. Inf. Commun. Technol.* **2003**, *50*, 105–112.
16. Bhamidipati, S.; Mina, T.; Gao, G. A Case Study Analysis for Designing a Lunar Navigation Satellite System with Time-Transfer from Earth-GPS. In Proceedings of the 34th International Technical Meeting of ION GNSS+, Online, 20–24 September 2021; pp. 950–965.
17. Shin, M.Y.; Park, C.; Lee, S.J. Atomic clock error modeling for GNSS software platform. In Proceedings of the IEEE/ION Position, Location and Navigation Symposium, Monterey, CA, USA, 5–8 May 2008; pp. 71–76. [CrossRef]
18. Galleani, L.; Tavella, P. Time and the Kalman Filter. *IEEE Control. Syst. Mag.* **2010**, *30*, 44–65.
19. Willner, D.; Chang, C.; Dunn, K. Kalman filter algorithms for a multi-sensor system. In Proceedings of the 1976 IEEE Conference on Decision and Control including the 15th Symposium on Adaptive Processes, Clearwater, FL, USA, 1–3 December 1976; pp. 570–574. [CrossRef]